# Age-of-Information in First-Come-First-Served Wireless Communications: Upper Bound and Performance Optimization

Wensheng Lin, *Member, IEEE*, Lixin Li, *Member, IEEE*, Jinhong Yuan, *Fellow, IEEE*, Zhu Han, *Fellow, IEEE*, Markku Juntti, *Fellow, IEEE*, and Tad Matsumoto, *Life Fellow, IEEE*

***Abstract*—This paper establishes an analytical framework for the upper bound on the average Age-of-Information (AoI) in first-come-first-served (FCFS) wireless communications where a certain level of outage probability is unavoidable. To begin with, we analyze the average AoI and derive a general upper bound for G/G/1 systems with a certain outage probability. Subsequently, for an M/M/1 system with the FCFS scheme, we obtain a concise closed-form expression of the upper bound, and further refine the upper bound after analyzing the relative error. Interestingly, it is found by the analysis that the relative error is independent of the service rate, and the upper bound becomes tighter as the outage probability increases. Based on the refined upper bound, we minimize the average AoI for the communications suffering from block Rayleigh fading. We derive a closed-form expression of the outage probability over a fading channel, and then prove that the refined upper bound is a convex function with respect to the average update generating rate. Consequently, we optimize the AoI performance by solving a convex optimization problem formulated utilizing the refined upper bound expression. The numerical results indicate that the minimum average AoI can be reduced by either increasing the service rate or the transmission power.**

***Index Terms*—Age-of-Information, outage probability, first-come-first-served, G/G/1 systems, M/M/1 systems.**

## I. Introduction

Age-of-Information (AoI) [1] is a reasonable metric indicating the dynamics of information freshness. Kaul *et al.* proposed the concept of AoI for the first time in [2], where AoI is introduced for designing transmission strategy in vehicular networks. The general definition of AoI is the elapsed time of the latest successfully updated information since the information is generated. Compared to static metrics such as delay and latency, AoI better reflects the variation of the information freshness along with time. Therefore, the concept of AoI has been widely adopted in various areas of network design as the key metric for performance analysis and/or algorithm design [3]–[7].

Nowadays, mobile devices have been and will be rapidly increasing as reported in [8], especially as Internet-of-Things (IoT) spreads over the world. The wireless transmissions may fail if the system suffers from severe fading and interference, resulting in the outage events which cannot be completely avoided because propagation of the electronic-magnetic waves is a natural phenomenon. Furthermore, in wireless IoT networks massive devices are assumed to be connected. Therefore, when using AoI as a metric for evaluating the performance of the wireless IoT networks, not only the latency due to the elapsed time in the queue but also the outage probability of the wireless links suffering from the fading variation, have to be taken into account. Once an outage event occurs, AoI increases continuously due to the failure of updating information. For the purpose of analyzing AoI in wireless communication networks, we need to establish a mathematical relationship between the outage probability and the average AoI.

In the IoT era, a lot of wireless devices rely on battery rather than power supply line during most of time (in fact, assuming power supply line contradicts wireless communications, because they can also guarantee reliable wired communications by cables). Hence, there is a constraint on the total transmission energy during a specific time interval for wireless devices. Then, an interesting trade-off appears, i.e., the system can increase the generating rate of updates to reduce AoI; however, more updates decrease the average transmission power and increase the outage probability, which causes larger AoI. To achieve the best trade-off between the generating rate of updates and the transmission power, it is necessary to derive the outage probability for a given transmission power in addition to the average AoI with a certain outage probability.

To date, there is some research work related to AoI analysis considering packet errors with a certain outage probability. The peak AoI for the M/M/1 system was characterized for the first-come-first-served (FCFS) or last-come-first-served (LCFS) scheme by Chen and Huang in [9]. Arafa *et al.* [10] analyzed the average AoI in energy harvesting communications where energy arrives according to a Poisson process and a status update is served immediately. Kam *et al.* [11] studied the average AoI for an M/M/1/2 system where the outage event is



This work was supported in part by National Natural Science Foundation of China (NSFC) under Grant 62001387, in part by Shanghai Academy of Spaceflight Technology (SAST) under Grant SAST2020124, in part by French National Research Agency Future program under reference ANR-10-LABX-07-01, in part by NSF CNS-2107216 and CNS-2128368, in part by the Australian Research Council (ARC) Discovery Projects under Grant DP190101363, in part by the ARC Linkage Project under Grant LP170101196, and in part by the Academy of Finland 6G Flagship program under Grant 346208.

Corresponding author: Wensheng Lin.

W. Lin and L. Li are with the School of Electronics and Information, Northwestern Polytechnical University, Xi'an, Shaanxi 710129, China (e-mail: linwest@nwpu.edu.cn; lilixin@nwpu.edu.cn).

J. Yuan is with the School of Electrical Engineering and Telecommunications, University of New South Wales, Sydney, NSW 2052, Australia (e-mail: j.yuan@unsw.edu.au).

Z. Han is with the Department of Electrical and Computer Engineering at the University of Houston, Houston, TX 77004 USA, and also with the Department of Computer Science and Engineering, Kyung Hee University, Seoul 446-701, South Korea (e-mail: zhan2@uh.edu).

M. Juntti is with the Centre for Wireless Communications, University of Oulu, 90014 Oulu, Finland (e-mail: markku.juntti@oulu.fi).

T. Matsumoto is with IMT Atlantique Bretagne Pays de la Loire, 4 Rue Alfred Kastler, 44300 Nantes, France. He is also Professor Emeritus of Japan Advanced Institute of Science and Technology, Japan (e-mail: matumoto@jaist.ac.jp), and University of Oulu, Finland.

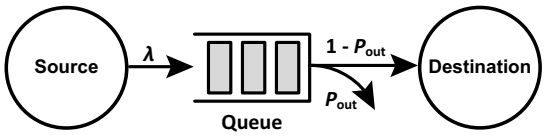


(a) Single source model (direct).

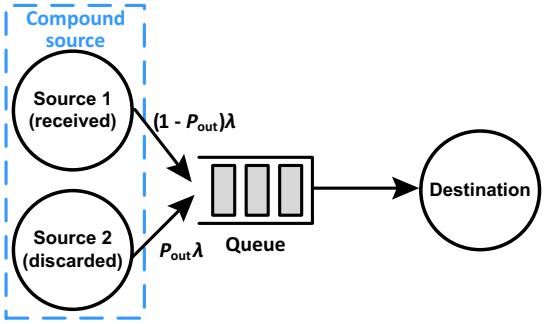


(b) multiple sources model (equivalent).

Fig. 1. Two ways to analyzing the AoI in communications with outages.

controlled by a packet deadline. Zhang *et al.* [12] minimized the total AoI by joint sensing and transmission optimization, taking into account the successful sensing probability. Lin *et al.* [13] derived a lower bound on the average AoI for the M/M/1 system with a given outage probability. Ling *et al.* [14] minimized the average discrete AoI in healthcare IoT with the outage probabilities of energy harvesting and information transmissions.

Nonetheless, it is not easy to obtain an exact expression of the average AoI for the general queueing model (i.e., the G/G/1 system) with the FCFS scheme, due to the complicated stochastic properties and the infinite queue length in various queueing models. The complicated calculation of the exact average AoI may hinder the practical implementation of some algorithms based on AoI. Therefore, the objective of this paper is to find a concise approximation (i.e., an upper bound) of the average AoI for G/G/1 systems with the FCFS scheme. By utilizing the upper bound, we can reduce the computation cost for AoI optimization while keeping the reasonable accuracy of the performance evaluation.

There are two ways to analyzing the AoI in wireless communications with outages, i.e., the direct and equivalent models as illustrated in Fig. 1(a) and Fig. 1(b), respectively. In the direct model, the source has an arrival rate $\lambda$, and the queue has a packet discard probability $P_{\text{out}}$. In the equivalent model, two sources have the arrival rates $(1-P_{\text{out}})\lambda$ and $P_{\text{out}}\lambda$, respectively. Hence, the arrival rate of the compound source is also equal to $\lambda$. If we only consider the AoI of Source 1 while ignoring Source 2, the result is equivalent to the direct model.

The previous results for the AoI analysis in the presence of multiple sources can be utilized for analyzing the AoI in communications with outages based on the equivalent model. Moltafet *et al.* [15] approximated the average AoI for the two sources M/G/1 system, which is equivalent to the system with outages by considering one of the sources as the discarded packet. Kaul and Yates [16] derived the average AoI for one of the sources in the multi-source M/M/1 system. Huang and Modiano [17] characterized the peak AoI for the two sources M/G/1 system.

However, a fundamental problem, arising when using the equivalent model, is how to construct the probability density functions (PDFs) of the information generation time interval for two sources, such that the PDF for the compound source is the same as the PDF for the source in the direct model. It is difficult to construct the PDFs for two sources unless the compound source follows a Poisson process. Due to the complexity of constructing the PDFs for two sources in G/G/1 systems, this paper analyzes AoI based on the direct model.

For the calculation of the outage probability, the scenario can be roughly classified into two categories: lossless and lossy communications. Actually, lossy communications reduce to lossless when the distortion requirement becomes 0, i.e., the recovered information is exactly the same as the source information. Hence, to make the results more generic, we derive the outage probability for lossy communications in this paper. The basic principle for the derivation of the outage probability is to calculate the probability of the instantaneous channel capacities less than the achievable capacities. Since the system models of cooperative communications have much more variety than that of point-to-point communications, the previous results regarding the outage probability are almost for cooperative communications. For example, Kramer *et al.* [18] determined the outage probability of lossless decode-and-forward (DF) relaying systems. As presented in [19]–[22], there were also a lot of work related to the outage probability analyses of lossless communications assisted by lossy-forward (LF) [23] relaying over block Rayleigh fading channels. Regarding end-to-end lossy communications, the outage probability was investigated for correlated binary sources in [24], [25].

Nevertheless, most of the previous work focuses on the outage probability for end-to-end lossless communications. Besides, the work for lossy communications analyzes the outage probability by numerical solutions instead of analytical solutions. Therefore, we aim at deriving a closed-form expression of the outage probability for lossy communications with a Gaussian source in this paper. By this means, we can further mathematically prove the optimality of the trade-off between the generating rate of updates and the transmission power for minimizing AoI.

Compared to the literature, this paper derives the upper bound on the average AoI for G/G/1 systems with the FCFS scheme, and determines the outage probability for lossy communications with a Gaussian source. Based on the closed-form expressions of the upper bound and the outage probability, the AoI performance is optimized for the system with an energy budget constraint. The contributions of this paper are summarized as follows:

- We establish an analytical framework for evaluating the average AoI for FCFS wireless communications with outages. Specifically, we derive an upper bound on the average AoI for the G/G/1 systems representing the most generic one-server queue model, given a required outage probability.

- We determine the upper bound on the average AoI for the M/M/1 system, and present a concise closed-form expression of the upper bound.
- We evaluate the relative error of the upper bound between the approximated and exact average AoI, and further propose a refined upper bound with a concise closed-form expression. The numerical results imply that the relative error is a function of the outage probability and the server utilization ratio.
- Based on the Shannon's lossy source-channel separation theorem [26], [27], we obtain a closed-form expression of the outage probability for point-to-point lossy communications with a Gaussian source over a block Rayleigh fading channel.
- Finally, we prove that the refined upper bound on the average AoI is a convex function with respect to the update generating rate. Hence, by utilizing the refined upper bound, the problem of minimizing the average AoI can be solved by the convex optimization framework. The numerical results demonstrate that the increment of the service rate or the transmission power efficiently reduces the minimum average AoI when they are within a relatively small range.

The rest of this paper is organized as follows. Section II establishes the analytical framework of the upper bound on the average AoI for FCFS communications with a certain level of outage probability. Section III derives an upper bound and refines the upper bound for the M/M/1 system. Section IV focuses on the AoI optimization for lossy communications with a Gaussian source over a block Rayleigh fading channel. Finally, we conclude this work in Section V.

## II. Analytical Framework of AoI in G/G/1 Systems

This section establishes the analytical framework of the average AoI and derives the upper bound for G/G/1 systems with a given outage probability.

We start with a brief review of the basic analytical framework on the average AoI for the G/G/1 system with the FCFS scheme in Section II-A. Then, we make an in-depth investigation on the dynamics of AoI when outage events occur in Section II-B. Section II-C presents a general upper bound on the average AoI with a given outage probability requirement.

### A. Basic Analytical Framework

Fig. 2 depicts the dynamics of AoI along with time elapsing for reliable communications. The $i$-th update is generated and its service is completed at the time of $t_i$ and $t'_i$, respectively. Therefore, $Y_i = t_i - t_{i-1}$ is the interarrival time between the $(i-1)$-th and the $i$-th updates. Moreover, the system time $T_i = t'_i - t_i$ is the period of time for the $i$-th update staying in the system. From the view of queueing process, the system time $T_i$ is the sum of the waiting time $W_i$ in the queue and the service time $S_i$, i.e., $T_i = W_i + S_i$. The $i$-th update has to wait from $t_i$ to $t'_{i-1}$, if it is generated before the system finishes the service of the $(i-1)$-th update; otherwise, the waiting time in the queue for the $i$-th update is 0. Hence, $W_i = (t'_{i-1} - t_i)^+ = (T_{i-1} - Y_i)^+$, where $(\cdot)^+ = \max(\cdot, 0)$.

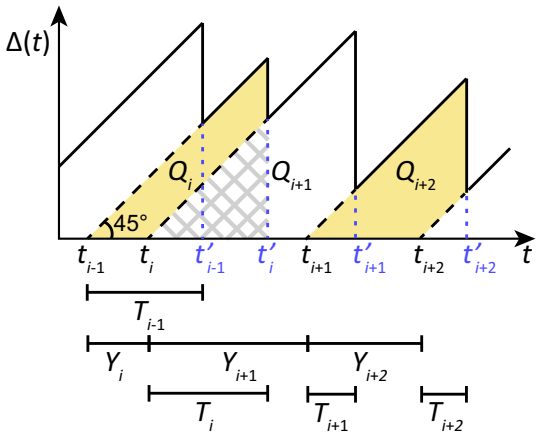


Fig. 2. The basic analytical framework of AoI for reliable communications.

Since the AoI $\Delta(t)$ is defined as the elapsed time of the latest served update from its generation, AoI will linearly increase along with time $t$ with a gradient of 1. The average AoI for an interval $(0, \mathcal{T})$ can be calculated by

$$\Delta_{\mathcal{T}} = \frac{1}{\mathcal{T}} \int_0^{\mathcal{T}} \Delta(t) dt, \tag{1}$$

where the integral is equal to the area under $\Delta(t)$. As $\mathcal{T} \to \infty$, $\Delta_{\mathcal{T}}$ converges into the average AoI $\Delta$ for the system in stable states. By decomposing the area under $\Delta(t)$ into the trapezoids with their area being $Q_i$, the average AoI $\Delta$ can be calculated as the expectation of $Q$ divided by the expectation of $Y$ [28, Eq. (2.12)], i.e., $\Delta = \frac{\mathrm{E}[Q]}{\mathrm{E}[Y]}$. The area $Q_i$ of a trapezoid is equal to the difference between two triangles, i.e.,

$$Q_i = \frac{1}{2}(Y_i + T_i)^2 - \frac{1}{2}T_i^2 = Y_i T_i + \frac{1}{2}Y_i^2. \tag{2}$$

Hence, we have

$$\Delta = \frac{\mathrm{E}[YT] + \mathrm{E}[Y^2]/2}{\mathrm{E}[Y]}. \tag{3}$$

### B. AoI with Outage Events

Now, we start the analysis of the AoI dynamics for the system where the outage events occur. As illustrated in Fig. 3, we consider the general case where the outage events occur $k$ times successively. In this case, $\Delta(t)$ monotonically increases from $t'_{i-1}$ to $t'_{i+k}$, and the system completes the service at the timing for the $(k+1)$ updates. Similar to the basic analytical framework of AoI for reliable communications, we can calculate the average AoI with $k$ outage events by defining auxiliary variables

$$\tilde{Y}_i = \sum_{j=i}^{i+k} Y_j, \tag{4}$$

$$\tilde{T}_i = T_{i+k}. \tag{5}$$

Then, the area $\tilde{Q}_i$ of the trapezoid with $k$ outage events can be calculated by

$$\tilde{Q}_i = \tilde{Y}_i \tilde{T}_i + \frac{1}{2}\tilde{Y}_i^2, \tag{6}$$

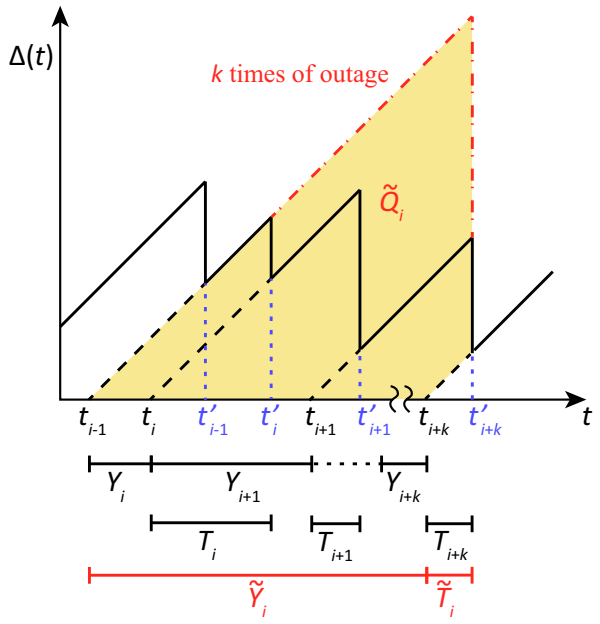


Fig. 3. The analytical framework of AoI with outage events.

and we can obtain the average AoI with $k$ outage events as

$$\Delta_{(k)} = \frac{\mathrm{E}[\tilde{Q}]}{\mathrm{E}[\tilde{Y}]} = \frac{\mathrm{E}[\tilde{Y}\tilde{T}] + \mathrm{E}[\tilde{Y}^2]/2}{\mathrm{E}[\tilde{Y}]}, \tag{7}$$

with

$$\mathrm{E}[\tilde{Y}\tilde{T}] = \sum_{j=i}^{i+k} \mathrm{E}[Y_j W_{i+k}] + (k+1)\mathrm{E}[Y]\mathrm{E}[S], \tag{8}$$

$$\mathrm{E}[\tilde{Y}^2] = (k+1)\left(\mathrm{E}[Y^2] + k(\mathrm{E}[Y])^2\right), \tag{9}$$

$$\mathrm{E}[\tilde{Y}] = (k+1)\mathrm{E}[Y]. \tag{10}$$

The calculations for (8)-(10) are presented in Appendix A.

Subsequently, given an outage probability, the average AoI of the overall system can be calculated by the following proposition.

*Proposition 1*: The average AoI of the overall system with an outage probability $P_{\text{out}}$ is

$$\Delta = (1 - P_{\text{out}})^2 \sum_{k=0}^{\infty} P_{\text{out}}^k (k+1)\Delta_{(k)}. \tag{11}$$

The proof of *Proposition 1* is presented in Appendix B.

From (7)-(10), we can find that the key to the calculation of the average AoI $\Delta$ is to determine $\mathrm{E}[Y_j W_{i+k}]$ in (8), since all other terms can be easily calculated given a specified queueing model. By contrast, $Y_j$ and $W_{i+k}$ are not independent for $j \leq i+k$ in general. Because the $j$-th update is generated earlier if the interarrival $Y_j$ decreases, and hence the $(i+k)$-th update also arrives earlier. However, the system requires the same time to finish the services of the updates, resulting in longer waiting time $W_{i+k}$. Therefore, $W_{i+k}$ has a higher probability to be larger for smaller $Y_j$. Since it is difficult to obtain the conditional PDF of $W_{i+k}$ for given $y_j$ (i.e., an instance of the random variable $Y_j$), we need to further decompose $\mathrm{E}[Y_j W_{i+k}]$ for calculating the exact value of $\Delta_{(k)}$. Consider

$$\begin{aligned}
&\mathrm{E}[Y_j W_{i+k}] \\
&= \mathrm{E}[Y_j (T_{i+k-1} - Y_{i+k})^+] \\
&= \mathrm{E}[Y_j (W_{i+k-1} + S_{i+k-1} - Y_{i+k})^+] \\
&= \mathrm{E}[Y_j ((T_{i+k-2} - Y_{i+k-1})^+ + S_{i+k-1} - Y_{i+k})^+] \\
&= \mathrm{E}[Y_j ((\cdots((T_{j-1} - Y_j)^+ + S_j - Y_{j+1})^+ + \cdots)^+ \\
&\quad + S_{i+k-1} - Y_{i+k})^+],
\end{aligned} \tag{12}$$

where all the variables in (12) are independent with each other, and (12) can be further calculated by the integral as

$$\begin{aligned}
\mathrm{E}[Y_j W_{i+k}] = \int_0^\infty \cdots \int_0^\infty & [y_j ((\cdots((t_{j-1} - y_j)^+ + s_j \\
& - y_{j+1})^+ + \cdots)^+ + s_{i+k-1} - y_{i+k})^+] \\
& \cdot f_T(t_{j-1}) f_Y(y_{i+k}) \prod_{m=j}^{i+k-1} f_S(s_m) f_Y(y_m) \\
& \cdot dt_{j-1} ds_j dy_j \cdots ds_{i+k-1} dy_{i+k-1} dy_{i+k}.
\end{aligned} \tag{13}$$

Notice that it is difficult to obtain a concise closed-form expression of (13). Alternatively, we can utilize numerical algorithms to calculate $\mathrm{E}[Y_j W_{i+k}]$.

For the purpose of AoI optimization, we derive an upper bound on the average AoI in the following. Here, we start with bounding $\Delta_{(k)}$. As derived above, the key to bounding $\Delta_{(k)}$ is to bound $\mathrm{E}[Y_j W_{i+k}]$, i.e., the term which is difficult to have a closed-form expression.

### C. General Upper Bound

We introduce the key results related to the upper bound first by the following two propositions.

*Proposition 2*: $\mathrm{E}[Y_j W_{i+k}]$ is upper bounded by

$$\mathrm{E}[Y_j W_{i+k}] < \mathrm{E}[Y_j W_{i-1}]. \tag{14}$$

The proof of *Proposition 2* is presented in Appendix C.

*Proposition 3*: $\Delta_{(k)}$ is upper bounded by

$$\Delta_{(k)} < \Delta_{(k)}^{\text{UB}} = \mathrm{E}[T] + \frac{\mathrm{E}[Y^2]}{2\mathrm{E}[Y]} + \frac{k\mathrm{E}[Y]}{2}. \tag{15}$$

*Proof.* Consider

$$\mathrm{E}[Y_j W_{i-1}] = \mathrm{E}[Y_j]\mathrm{E}[W_{i-1}] = \mathrm{E}[Y]\mathrm{E}[W], \tag{16}$$

where (16) follows since $j > i-1$ and hence $W_{i-1}$ is independent of $Y_j$. By substituting (14) and (16) into (8), we have

$$\begin{aligned}
\mathrm{E}[\tilde{Y}\tilde{T}] &< \sum_{j=i}^{i+k} \mathrm{E}[Y]\mathrm{E}[W] + (k+1)\mathrm{E}[Y]\mathrm{E}[S] \\
&= (k+1)\mathrm{E}[Y]\mathrm{E}[W] + (k+1)\mathrm{E}[Y]\mathrm{E}[S] \\
&= (k+1)\mathrm{E}[Y](\mathrm{E}[W] + \mathrm{E}[S]) \\
&= (k+1)\mathrm{E}[Y]\mathrm{E}[T].
\end{aligned} \tag{17}$$

Then, we combine (7), (9), (10) and (17) together to upper bound $\Delta_{(k)}$ as

$$\Delta_{(k)} < \frac{(k+1)\mathrm{E}[Y]\mathrm{E}[T] + (k+1)\left(\mathrm{E}[Y^2] + k(\mathrm{E}[Y])^2\right)/2}{(k+1)\mathrm{E}[Y]}$$

$$= \mathrm{E}[T] + \frac{\mathrm{E}[Y^2]}{2\mathrm{E}[Y]} + \frac{k\mathrm{E}[Y]}{2}. \tag{18}$$

This finishes the proof of *Proposition 3*. ■

Consequently, we can substitute $\Delta_{(k)}^{\mathrm{UB}}$ into (11) to obtain the upper bound on the average AoI for the system with outage events.

## III. AoI Analysis for M/M/1 Systems

In order to visually evaluate the AoI performance, we need to specify the queueing model of the system. Thus, we select the most fundamental model, i.e., the M/M/1 system for performance analysis. The arrival of updates follows a Poisson process with mean arrival rate $\lambda$, and the service time follows the exponential distribution with parameter $\mu$. Section III-A derives a concise closed-form expression of the upper bound on the average AoI in the M/M/1 system with outage events for the first step. Subsequently, Section III-B evaluates the relative error of the upper bound, and then refines the upper bound. Finally, Section III-C presents the numerical results with respect to the upper bound.

### A. Upper Bound Derivation

For better reference, we summarize the PDFs and the expectations of basic variables in the M/M/1 system with the FCFS scheme as follows.

- Since the arrival of updates follows a Poisson process with mean arrival rate $\lambda$, the interarrival $Y$ follows the independent and identically distributed (i.i.d.) exponential distribution with parameter $\lambda$, i.e.,

$$f_Y(y) = \lambda e^{-\lambda y}, 0 \le y, \tag{19}$$

$$\mathrm{E}[Y] = \frac{1}{\lambda}. \tag{20}$$

- The PDF and the expectation of the system time $T$ are given by [29, Eq. (16-97), (16-98)]

$$f_T(t) = \mu(1-\rho)e^{-\mu(1-\rho)t} = (\mu-\lambda)e^{-(\mu-\lambda)t}, 0 \le t, \tag{21}$$

$$\mathrm{E}[T] = \frac{1}{\mu(1-\rho)} = \frac{1}{\mu-\lambda}, \tag{22}$$

where $\mu$ is the service rate and $\rho = \frac{\lambda}{\mu}$ is the server utilization ratio.

To calculate the upper bound for the M/M/1 system, we consider

$$\begin{aligned}\mathrm{E}[Y^2] &= \int_0^\infty y^2 \lambda e^{-\lambda y} dy \\ &= \lambda e^{-\lambda y}\left(-\frac{y^2}{\lambda} - \frac{2y}{\lambda^2} - \frac{2}{\lambda^3}\right)\Big|_0^\infty \qquad (23)\\ &= \frac{2}{\lambda^2}, \qquad (24)\end{aligned}$$

where (23) follows according to [30, Eq. (2.322.2)].

By substituting (20), (22) and (24) into (15), we have

$$\Delta_{(k)}^{\mathrm{UB}} = \frac{1}{\mu-\lambda} + \frac{2/\lambda^2}{2/\lambda} + \frac{k/\lambda}{2} = \frac{1}{\mu-\lambda} + \frac{1}{\lambda} + \frac{k}{2\lambda}, \tag{25}$$

which can be further substituted into (11) to upper bound the average AoI for the system with outage events as

$$\begin{aligned}\Delta^{\mathrm{UB}} &= (1-P_{\mathrm{out}})^2 \sum_{k=0}^{\infty} P_{\mathrm{out}}^k (k+1)\Delta_{(k)}^{\mathrm{UB}} \qquad (26)\\ &= (1-P_{\mathrm{out}})^2 \sum_{k=0}^{\infty} P_{\mathrm{out}}^k (k+1)\left(\frac{1}{\mu-\lambda} + \frac{1}{\lambda} + \frac{k}{2\lambda}\right)\\ &= (1-P_{\mathrm{out}})^2 \sum_{k=0}^{\infty} P_{\mathrm{out}}^k (k+1)\left(\frac{1}{\mu-\lambda} + \frac{1}{\lambda}\right)\\ &\quad + (1-P_{\mathrm{out}})^2 \sum_{k=0}^{\infty} P_{\mathrm{out}}^k (k+1)\frac{k}{2\lambda}\\ &= \frac{1}{\mu-\lambda} + \frac{1}{\lambda} + \frac{(1-P_{\mathrm{out}})^2}{2\lambda} \sum_{k=0}^{\infty} P_{\mathrm{out}}^k k(k+1), \qquad (27)\end{aligned}$$

where (27) follows according to [30, Eq. (0.231.2)] for $P_{\mathrm{out}} < 1$.

In order to calculate $\sum_{k=0}^{\infty} P_{\mathrm{out}}^k k(k+1)$, let $\zeta = \sum_{k=0}^{\infty} P_{\mathrm{out}}^k \cdot k(k+1)$ and consider

$$\zeta P_{\mathrm{out}} = \sum_{k=0}^{\infty} P_{\mathrm{out}}^{k+1} k(k+1) = \sum_{k=1}^{\infty} P_{\mathrm{out}}^k (k-1)k. \tag{28}$$

Then, we have

$$\begin{aligned}\zeta(1-P_{\mathrm{out}}) &= \zeta - \zeta P_{\mathrm{out}}\\ &= \sum_{k=0}^{\infty} P_{\mathrm{out}}^k k(k+1) - \sum_{k=1}^{\infty} P_{\mathrm{out}}^k (k-1)k\\ &= \sum_{k=1}^{\infty} P_{\mathrm{out}}^k [k(k+1) - (k-1)k]\\ &= \sum_{k=1}^{\infty} 2k P_{\mathrm{out}}^k\\ &= \frac{2P_{\mathrm{out}}}{(1-P_{\mathrm{out}})^2}, \qquad (29)\end{aligned}$$

where (29) follows according to [30, Eq. (0.231.2)] for $P_{\mathrm{out}} < 1$. Hence, we can obtain

$$\sum_{k=0}^{\infty} P_{\mathrm{out}}^k k(k+1) = \zeta = \frac{2P_{\mathrm{out}}}{(1-P_{\mathrm{out}})^3}. \tag{30}$$

By substituting (30) into (27), we can obtain the closed-form expression of the upper bound as

$$\begin{aligned}\Delta^{\mathrm{UB}} &= \frac{1}{\mu-\lambda} + \frac{1}{\lambda} + \frac{(1-P_{\mathrm{out}})^2}{2\lambda} \cdot \frac{2P_{\mathrm{out}}}{(1-P_{\mathrm{out}})^3}\\ &= \frac{1}{\mu-\lambda} + \frac{1}{\lambda} + \frac{P_{\mathrm{out}}}{\lambda(1-P_{\mathrm{out}})}\\ &= \frac{1}{\mu-\lambda} + \frac{1}{\lambda(1-P_{\mathrm{out}})}. \qquad (31)\end{aligned}$$

*Remark:* $\Delta^{\mathrm{UB}}$ is an increasing function of $P_{\mathrm{out}}$. This matches our intuition that the average AoI increases as $P_{\mathrm{out}}$ goes larger.

### B. Relative Error and Refined Upper Bound

The relative error between the upper bound and the exact value of the average AoI is defined by

$$err = \frac{\Delta^{\mathrm{UB}} - \Delta}{\Delta}. \tag{32}$$

When $k = 0$, the exact value of the average AoI $\Delta_{(0)}$ is given by [28, Eq. (2.19)]

$$\Delta_{(0)} = \frac{1}{\mu}\left(1 + \frac{1}{\rho} + \frac{\rho^2}{1-\rho}\right). \tag{33}$$

Therefore, we can calculate the relative error between the upper bound and the exact value of the average AoI for $k = 0$ as

$$\begin{aligned} err_{(0)} &= \frac{\Delta_{(0)}^{\mathrm{UB}} - \Delta_{(0)}}{\Delta_{(0)}} \\ &= \frac{\left[\frac{1}{\mu-\lambda} + \frac{1}{\lambda} + \frac{0}{2\lambda} - \frac{1}{\mu}\left(1 + \frac{1}{\rho} + \frac{\rho^2}{1-\rho}\right)\right]}{\left[\frac{1}{\mu}\left(1 + \frac{1}{\rho} + \frac{\rho^2}{1-\rho}\right)\right]} \\ &= \frac{1}{1-\rho^2+\rho^3} - 1. \end{aligned} \tag{34}$$

Notice that when $P_{\mathrm{out}} = 0$, the average AoI for the system with outage events in (11) reduces to the average AoI without outage events. Hence, (34) is the relative error of the upper bound on the average AoI for reliable communications. For $k > 0$, since the exact expression of the average AoI is still an open problem, we need to utilize numerical results to evaluate the relative error of the upper bound.

Since we already know the exact expression of the average AoI for $k = 0$, we can replace $\Delta_{(0)}^{\mathrm{UB}}$ with $\Delta_{(0)}$ to reduce the relative error when calculating the upper bound from (26). Then, the refined upper bound is obtained from (11) as

$$\begin{aligned} \Delta^{\mathrm{UB}*} &= (1-P_{\mathrm{out}})^2\left[\sum_{k=0}^{\infty} P_{\mathrm{out}}^k (k+1)\Delta_{(k)}^{\mathrm{UB}} - \Delta_{(0)}^{\mathrm{UB}} + \Delta_{(0)}\right] \\ &= \Delta^{\mathrm{UB}} + (1-P_{\mathrm{out}})^2\left[-\Delta_{(0)}^{\mathrm{UB}} + \Delta_{(0)}\right] \qquad (35) \\ &= \frac{1}{\mu-\lambda} + \frac{1}{\lambda(1-P_{\mathrm{out}})} + (1-P_{\mathrm{out}})^2 \\ &\quad \cdot \left[-\frac{1}{\mu-\lambda} - \frac{1}{\lambda} + \frac{1}{\mu}\left(1 + \frac{1}{\rho} + \frac{\rho^2}{1-\rho}\right)\right] \\ &= \frac{1}{\mu-\lambda} + \frac{1}{\lambda(1-P_{\mathrm{out}})} - \frac{\lambda(1-P_{\mathrm{out}})^2}{\mu^2}. \qquad (36) \end{aligned}$$

### C. Numerical Results

*1) Upper Bound:* We evaluate the exact average AoI for the system with outage events by Monte Carlo simulation [31]. Fig. 4 compares the upper bound with the simulation results with respect to the average AoI. It is noticeable that the gap between the upper bound and the exact average AoI becomes smaller as the service rate $\mu$ increases. Interestingly, the gap seems not sensitive to the outage probability, i.e., the deviation degrees are similar even though $P_{\mathrm{out}}$ varies within a large range from 0 to 0.8.

Fig. 5 illustrates the curves of the refined upper bound. It is certain that the refined upper bound for $P_{\mathrm{out}} = 0$ should coincide with the exact average AoI without outage events. However, the improvement of the refined upper bound is not obvious for a large outage probability, because (35) indicates that the weight of $\Delta_{(0)}$ reduces as $P_{\mathrm{out}}$ increases. Therefore, the effect of refinement by replacing $\Delta_{(0)}^{\mathrm{UB}}$ with $\Delta_{(0)}$ also decreases if the outage probability becomes larger.

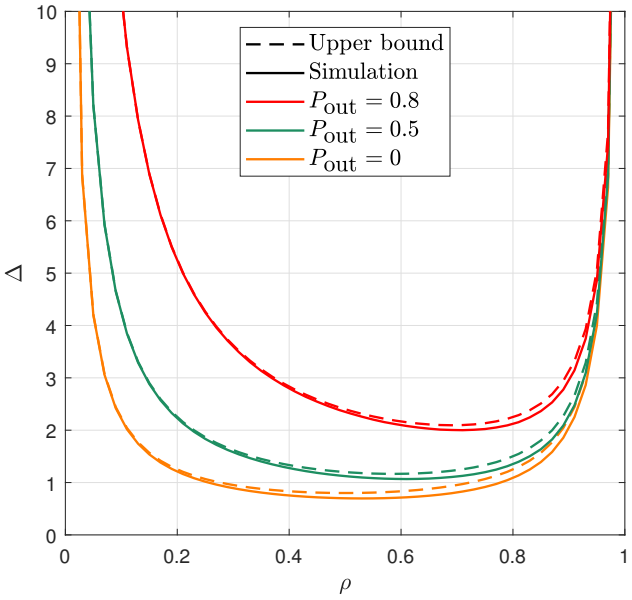


(a) $\mu = 5$.

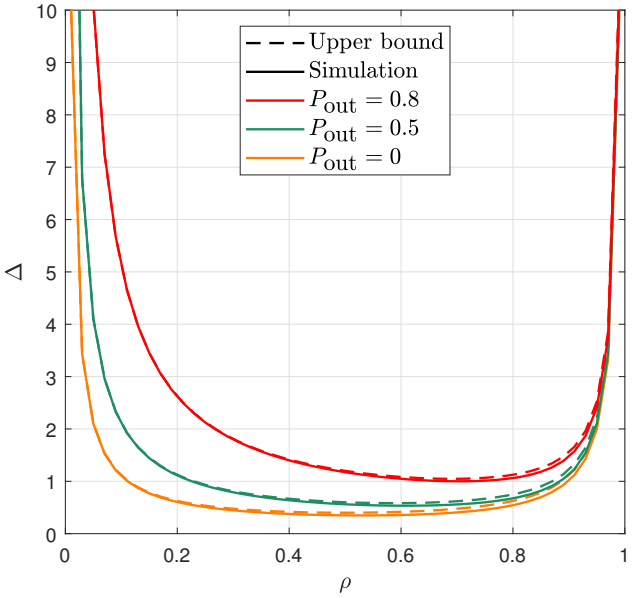


(b) $\mu = 10$.

Fig. 4. Upper bound on the average AoI.

*2) Relative Error:* As shown in Fig. 6, the relative errors of the upper bound and the refined upper bound are relatively small, and represent the tightness of the upper bound. Moreover, Fig. 6(a) demonstrates that the relative error decreases as the outage probability increases. This observation matches the phenomenon in Fig. 4 that the deviation degrees are similar for diverse $P_{\mathrm{out}}$, and hence the relative error decreases when the

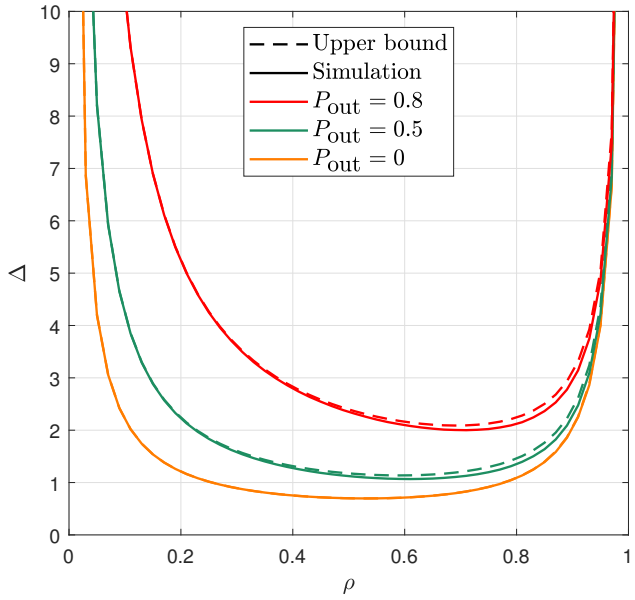


(a) $\mu = 5$.

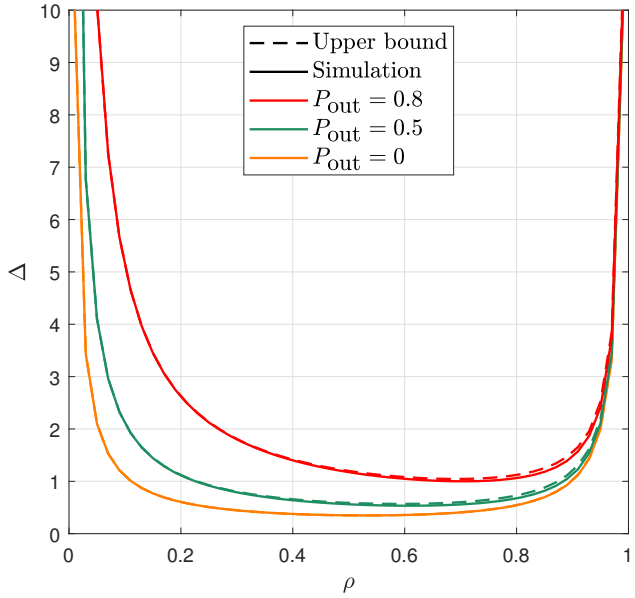


(b) $\mu = 10$.

Fig. 5. Refined upper bound on the average AoI.

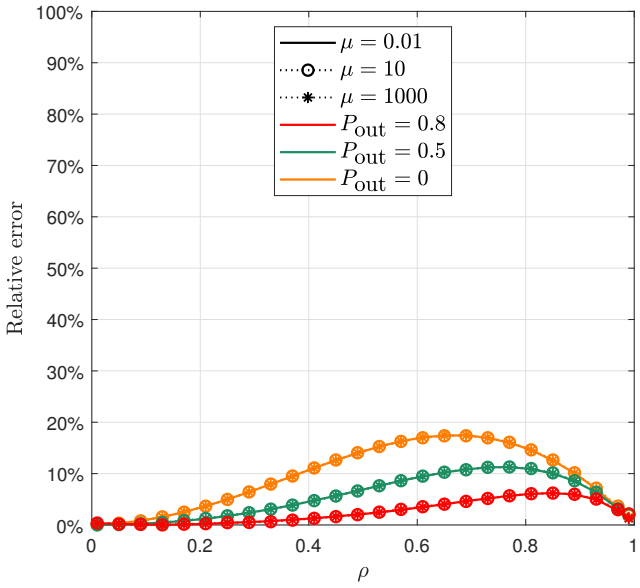


(a) Upper bound.

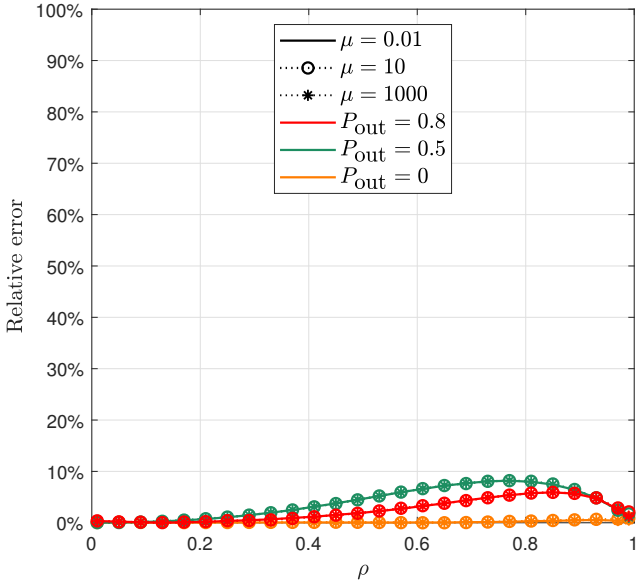


(b) Refined upper bound.

Fig. 6. Relative error of the upper bound.

average AoI increases for larger $P_{\text{out}}$. Interestingly, the curves completely coincide with each other for different $\mu$, even if $\mu$ is scaled by a huge degree, e.g., from 0.01 to 1000. This observation implies that the relative error is a function of $\rho$ and $P_{\text{out}}$ as denoted by $err(\rho, P_{\text{out}})$.

## IV. AoI Optimization

In this section, we optimize the average AoI based on the upper bound for a system with energy limitation. For simplicity, we consider a basic point-to-point lossy communication model with only one Gaussian source and one destination. Initially, the communication model is introduced in detail in Section IV-A. Then, Section IV-B derives a closed-form expression of the outage probability. In Section IV-C, we prove the convexity of the refined upper bound and utilize it for solving the optimal trade-off among the parameters related to the average AoI. The numerical results of AoI optimization are provided in Section IV-D.

### A. Communication Model

*1) System Model:* The M/M/1 system with the FCFS scheme has an i.i.d. Gaussian source $X \sim N(0, \sigma^2)$ generating information updates in the form of Gaussian sequences at the mean rate $\lambda$. In practical systems, the source could be a sensor, and hence we can control the generating rate $\lambda$ of updates. This fundamental assumption allows us to optimize the average AoI by adjusting $\lambda$. The update sequences are encoded, and then

continuously transmitted to a destination having a buffer with a sufficiently large size. Then, the destination processes the received update sequences at the mean service rate $\mu$. After decoding, the distortion of the reconstructed update sequence is evaluated, Gaussian symbol by symbol, by quadratic (squared error) distortion measure $d_{\mathrm{Q}}(x,\hat{x})=(x-\hat{x})^2$. If the average distortion of a reconstructed update sequence is larger than the specified distortion requirement $D$, the reconstructed update sequence is discarded and an outage event occur.

*2) Channel Model:* The transmissions are assumed to suffer from independent block Rayleigh fading. For a transmitted symbol $x_t$ with transmission power $P_t = \mathrm{E}\left[|x_t|^2\right]$, the received symbol $x_r$ is expressed by

$$x_r = \sqrt{G}hx_t + z, \tag{37}$$

where $G$ is the geometric gain dominated by the environment conditions and the locations of the source and the destination. $h$ represents the complex channel gain which is normalized to unity or $\mathrm{E}\left[|h|^2\right]=1$ for simplicity. $z$ stands for the zero-mean additive white Gaussian noise (AWGN) with its power spectral density being $N_0$. Then, the instantaneous signal-to-noise ratio (SNR) and the average SNR are given by

$$\gamma = \frac{G|h|^2P_t}{N_0}, \tag{38}$$

$$\overline{\gamma} = \frac{GP_t}{N_0}. \tag{39}$$

Obviously, $|h|^2=\frac{\gamma}{\overline{\gamma}}$, and hence the PDF of the instantaneous SNR for Rayleigh fading is

$$f_{\mathrm{SNR}}(\gamma) = \frac{1}{\overline{\gamma}}\exp\left(-\frac{\gamma}{\overline{\gamma}}\right). \tag{40}$$

### *B. Outage Probability*

To derive the outage probability, we need to determine the condition when the distortion requirement can be satisfied. According to [32, Theorem 10.3.2], the rate-distortion function of a Gaussian source $X\sim N(0,\sigma^2)$ for the distortion degree $D$ is given by

$$R(D) = \frac{1}{2}\log^+\left(\frac{\sigma^2}{D}\right), \tag{41}$$

where $\log^+(\cdot)=\max\{\log(\cdot),0\}$, and the base of logarithm function $\log(\cdot)$ is assumed to be 2 unless specified. Then, the Shannon's lossy source-channel separation theorem indicates that the distortions $D$ can be satisfied if [33, Theorem 3.7]

$$rR(D) \le C(\gamma), \tag{42}$$

where $r$ stands for the end-to-end rate of joint source-channel coding, and $C(\gamma)=\log(1+\gamma)$ is the Shannon capacity for two dimensional signaling using Gaussian codebook. Let $c=C(\gamma)$ be the instantaneous channel capacity, and then we have

$$\gamma = 2^c - 1. \tag{43}$$

Based on the concept of transformation of random variables [29, Chapter 5], the characteristic function of $c$ is given by [29, Eq. (5-114)]

$$\begin{aligned}\Phi_C(\omega) &= \int_{-\infty}^{\infty}\exp\left(j\omega C(\gamma)\right)\cdot f_{\mathrm{SNR}}(\gamma)d\gamma\\ &= \int_{-\infty}^{\infty}\exp\left(j\omega c\right)\cdot\frac{1}{\overline{\gamma}}\exp\left(-\frac{2^c-1}{\overline{\gamma}}\right)d(2^c-1)\\ &= \int_{-\infty}^{\infty}\exp\left(j\omega c\right)\cdot\frac{2^c\ln 2}{\overline{\gamma}}\exp\left(-\frac{2^c-1}{\overline{\gamma}}\right)dc.\end{aligned} \tag{44}$$

Hence, the PDF of the instantaneous channel capacity is

$$f_C(c) = \frac{2^c\ln 2}{\overline{\gamma}}\exp\left(-\frac{2^c-1}{\overline{\gamma}}\right). \tag{45}$$

Consequently, given a distortion requirement $D$, the outage probability can be calculated by the probability that the instantaneous channel capacity is less than $rR(D)$, i.e.,

$$\begin{aligned}P_{\text{out}} &= \int_0^{rR(D)} f_C(c)dc\\ &= \int_0^{rR(D)}\frac{2^c\ln 2}{\overline{\gamma}}\exp\left(-\frac{2^c-1}{\overline{\gamma}}\right)dc\\ &= -\exp\left(-\frac{2^c-1}{\overline{\gamma}}\right)\Bigg|_0^{rR(D)}\\ &= 1-\exp\left(-\frac{2^{rR(D)}-1}{\overline{\gamma}}\right)\\ &= 1-\exp\left(-\frac{\mathrm{pow}\left[2,\frac{r}{2}\log^+\left(\frac{\sigma^2}{D}\right)\right]-1}{\overline{\gamma}}\right)\\ &= 1-\exp\left(-\frac{\left[\left(\sigma^2/D\right)^{\frac{r}{2}}-1\right]^+}{\overline{\gamma}}\right),\end{aligned} \tag{46}$$

where $\mathrm{pow}(a,b)=a^b$.

### *C. AoI Minimization*

Assuming that $P_T$ is the total transmission energy in a unit of time, then $P_T/\lambda$ is the transmission power of each update for mean arrival rate being $\lambda$[1]. Therefore, the average SNR is

$$\overline{\gamma} = \frac{GP_T}{\lambda N_0}. \tag{47}$$

Then, we have

$$\begin{aligned}\Delta^{\mathrm{UB}*} &= \frac{1}{\mu-\lambda}+\frac{1}{\lambda}\exp\left(\frac{\left[\left(\sigma^2/D\right)^{\frac{r}{2}}-1\right]^+}{\overline{\gamma}}\right)-\frac{\lambda}{\mu^2}\\ &\quad\cdot\exp\left(-\frac{2\left[\left(\sigma^2/D\right)^{\frac{r}{2}}-1\right]^+}{\overline{\gamma}}\right)\\ &= \frac{1}{\mu-\lambda}+\frac{1}{\lambda}\exp\left(\frac{\lambda N_0\left[\left(\sigma^2/D\right)^{\frac{r}{2}}-1\right]^+}{GP_T}\right)\\ &\quad-\frac{\lambda}{\mu^2}\exp\left(-\frac{2\lambda N_0\left[\left(\sigma^2/D\right)^{\frac{r}{2}}-1\right]^+}{GP_T}\right)\end{aligned}$$

[1]Notice that the transmission power of each update increases as $\lambda$ decreases, and $P_T/\lambda$ goes extremely large if $\lambda$ tends to 0. However, practical systems may not support such a large transmission power. This limitation on the maximum transmission power can be considered as a constraint for AoI optimization in practical systems.

$$= \frac{1}{\mu-\lambda} + \frac{1}{\lambda}e^{\xi\lambda} - \frac{\lambda}{\mu^2}e^{-2\xi\lambda}, \tag{48}$$

where we define $\xi = \frac{N_0\left[\left(\sigma^2/D\right)^{\frac{r}{2}}-1\right]^+}{GP_T}$ for conciseness.

Now, we prove the convexity of $\Delta^{\mathrm{UB}*}$ below. Consider

$$\begin{aligned}\frac{\partial^2\Delta^{\mathrm{UB}*}}{\partial\lambda^2} &= \frac{2}{(\mu-\lambda)^3} + \frac{e^{\xi\lambda}}{\lambda^3}\left(\xi^2\lambda^2 - 2\xi\lambda + 2\right) \\ &\quad - \frac{4\xi e^{-2\xi\lambda}}{\mu^2}(\xi\lambda - 1) \\ &= \frac{2}{(\mu-\lambda)^3} + \frac{e^{\xi\lambda}}{\lambda^3}\left[(\xi\lambda-1)^2+1\right] \\ &\quad - \frac{4\xi e^{-2\xi\lambda}}{\mu^2}(\xi\lambda - 1). \end{aligned} \tag{49}$$

When $\xi\lambda - 1 \leq 0$, it is obvious that $\frac{\partial^2\Delta^{\mathrm{UB}*}}{\partial\lambda^2} > 0$ since $\mu > \lambda > 0$. When $\xi\lambda - 1 > 0$, we have $e^{\xi\lambda} > e$ and $e^{\xi\lambda} > \xi\lambda$. Then, consider

$$\begin{aligned}&\frac{e^{\xi\lambda}}{\lambda^3}\left[(\xi\lambda-1)^2+1\right] \\ &= \frac{e^{\xi\lambda}\cdot e^{2\xi\lambda}\cdot e^{-2\xi\lambda}}{\lambda\cdot\lambda^2}\left[(\xi\lambda-1)^2+1\right] \\ &> \frac{\xi\lambda\cdot e^2\cdot e^{-2\xi\lambda}}{\lambda\cdot\mu^2}\left[(\xi\lambda-1)^2+1\right] \\ &= \frac{\xi e^2\cdot e^{-2\xi\lambda}}{\mu^2}\left[\xi^2\lambda^2 - 3\xi\lambda + 3 + (\xi\lambda-1)\right] \\ &= \frac{\xi e^2\cdot e^{-2\xi\lambda}}{\mu^2}\left[\left(\xi\lambda-\frac{3}{2}\right)^2 + \frac{3}{4} + (\xi\lambda-1)\right] \\ &> \frac{4\xi e^{-2\xi\lambda}}{\mu^2}(\xi\lambda-1). \end{aligned} \tag{50}$$

By substituting (50) into (49), we can obtain $\frac{\partial^2\Delta^{\mathrm{UB}*}}{\partial\lambda^2} > 0$. Consequently, $\Delta^{\mathrm{UB}*}$ is a convex function with respect to $\lambda$, and we can minimize $\Delta^{\mathrm{UB}*}$ by convex optimization.

### *D. Numerical Results*

Fig. 7(a) and Fig. 7(b) illustrate the tendency of $\Delta^{\mathrm{UB}*}$ for diverse values of $\mu$ and $P_T$, respectively. Certainly, the average AoI and the minimum average AoI decrease as $\mu$ or $P_T$ increases. Nevertheless, the performance gain also decreases fast as $\mu$ or $P_T$ increases, especially when $\mu \geq 20$ and $P_T \geq 6$. This is because larger $\mu$ allows $\lambda$ to be larger to reduce the maximum AoI of each transmission. However, since the $P_T$ is fixed in Fig. 7(a), larger $\lambda$ reduces the transmission power resulting in a higher outage probability. When the transmission power decreases to a relatively small value, the outage probability becomes the dominant factor of the average AoI. Hence, it is difficult to further increase $\lambda$, and even larger $\mu$ can hardly affect the average AoI. For Fig. 7(b), larger $P_T$ allows $\lambda$ to increase for reducing the maximum AoI, while keeping the outage probability at a relatively low level. However, the optimal $\lambda$ is constrained by fixed $\mu$, i.e., $\lambda$ cannot increase arbitrarily. Therefore, when $P_T$ is sufficiently large, the outage probability already remains extremely low and it is difficult to obtain more gains. Another phenomenon is that when $P_T$ becomes sufficiently large, the outage probability keeps at almost 0 in spite of $\lambda$, and hence the curve of the average AoI has the same shape as the curve without outage events.

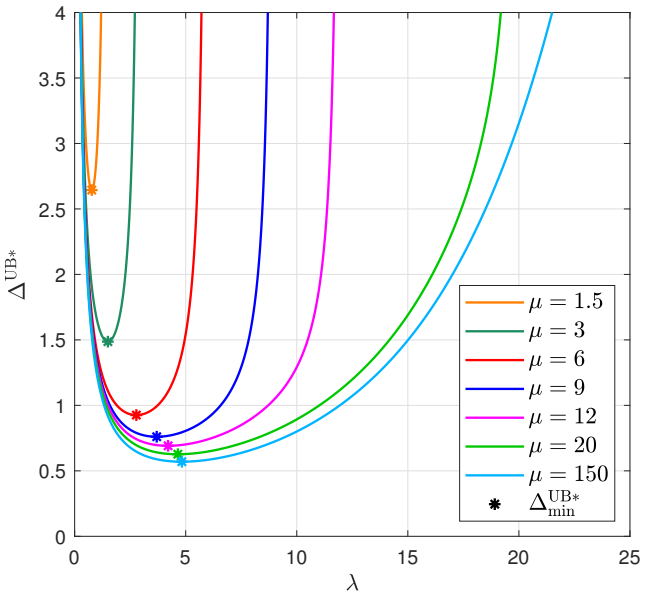


(a) $P_T = 2$.

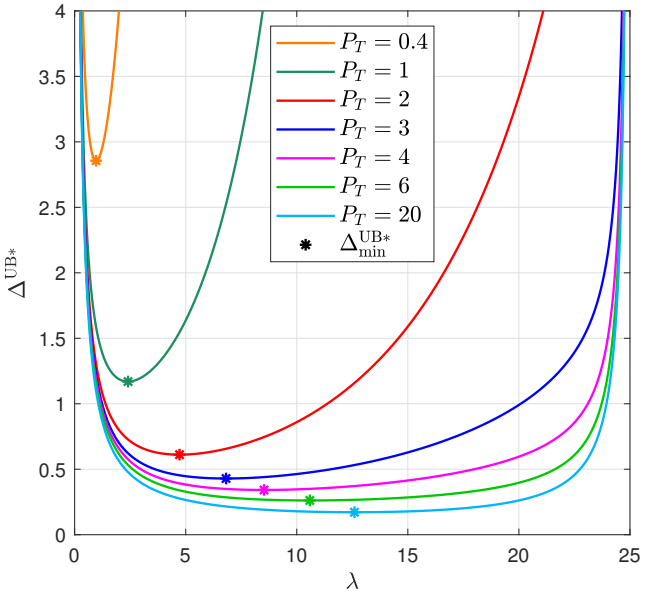


(b) $\mu = 25$.

Fig. 7. $\Delta^{\mathrm{UB}*}$ for $\sigma = 2, D = 2, N_0 = 1, G = 1$ and $r = 1$.

Fig. 8 depicts minimum $\Delta^{\mathrm{UB}*}$ for various distortion requirements. Clearly, the minimum average AoI decreases as the distortion requirement $D$ increases, because the outage probability is lower for less strict distortion requirements. Fig. 8(a) and Fig. 8(b) show that the minimum average AoI decreases slowly as $\mu$ and $P_T$ become relatively large, respectively. This observation matches the result in Fig. 7 as discussed above.

It is found from Fig. 9 that the minimum average AoI decreases rapidly when $D$ is small. This can be understood

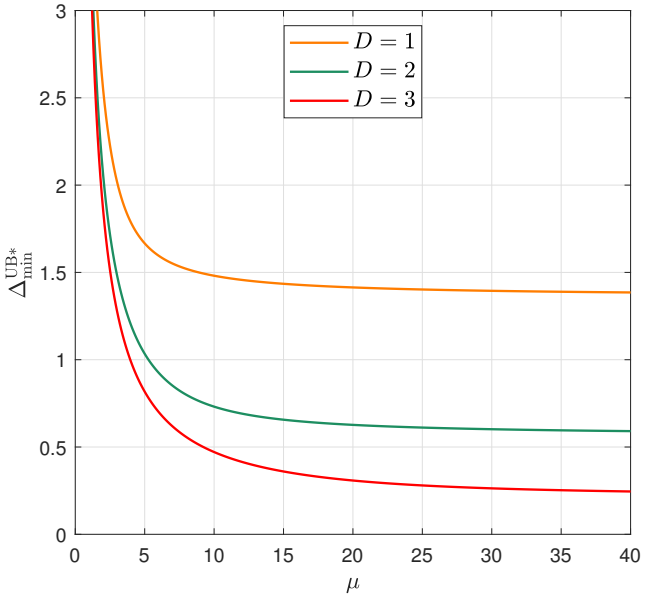


(a) $P_T = 2$.

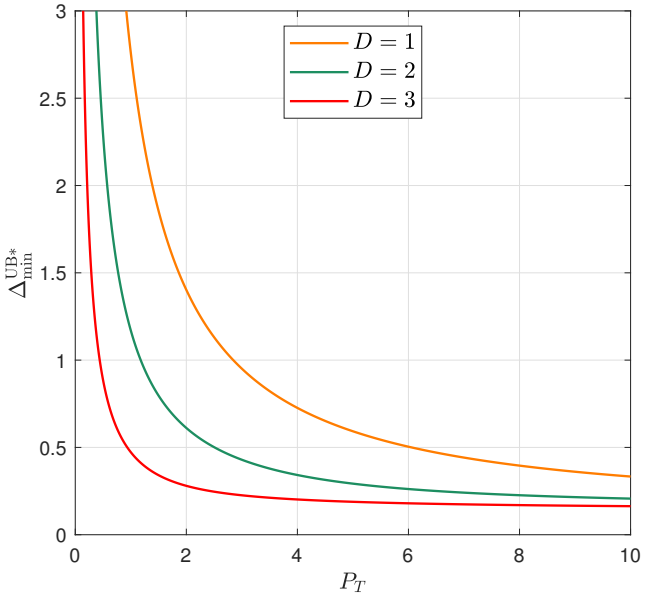


(b) $\mu = 25$.

Fig. 8. Minimum $\Delta^{\mathrm{UB}*}$ for $\sigma = 2, N_0 = 1, G = 1$ and $r = 1$.

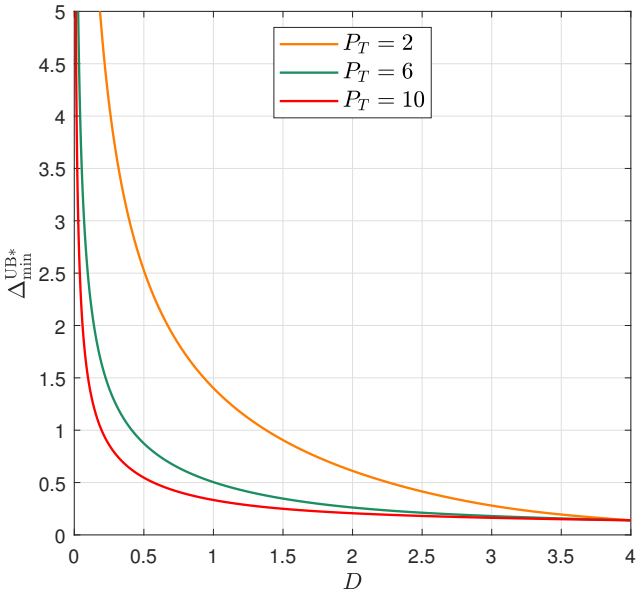


Fig. 9. Minimum $\Delta^{\mathrm{UB}*}$ for $\sigma = 2, N_0 = 1, G = 1, r = 1$ and $\mu = 25$.

from the rate-distortion function that small $D$ requires an extremely high rate, resulting in a very large outage probability. Moreover, the minimum average AoI finally converges together when $D = \sigma^2 = 4$. This is because $D \geq \sigma^2$ can be always satisfied with the Gaussian source at the zero source coding rate, which means that the outage event will never occur regardless of $P_T$.

## V. Conclusion

In this paper, we have established an analytical framework of the upper bound on the average AoI in outage-acceptable G/G/1 systems with the FCFS scheme. We, first of all, characterized a general upper bound on the average AoI for a specified outage probability. Then, we conducted the AoI analysis for the M/M/1 system, and we obtained a concise closed-form expression of the upper bound on the average AoI. We also evaluated the relative error of the upper bound, and further proposed a refined upper bound on the average AoI. Furthermore, we derived a closed-form expression of the outage probability for point-to-point lossy communications with a Gaussian source suffering from block Rayleigh fading. We proved the convexity of the refined upper bound on the average AoI with respect to the generating rate of updates. With the convex optimization framework based on the refined upper bound, we identified the trade-off between the generating rate of updates and the transmission power for minimizing the average AoI. The numerical results indicate that if either $\mu$ or $P_T$ is fixed, the performance gain in terms of the reduction of minimum average AoI is extremely small even when the unfixed parameter becomes large.

## Appendix A
## Calculations for (8)-(10)

$$\begin{aligned}
\mathrm{E}[\tilde{Y}\tilde{T}] &= \mathrm{E}[\tilde{Y}_i\tilde{T}_i] \\
&= \mathrm{E}\left[\left(\sum_{j=i}^{i+k} Y_j\right) \cdot T_{i+k}\right] \\
&= \sum_{j=i}^{i+k} \mathrm{E}[Y_j T_{i+k}] \\
&= \sum_{j=i}^{i+k} \mathrm{E}[Y_j (W_{i+k} + S_{i+k})] \\
&= \sum_{j=i}^{i+k} \mathrm{E}[Y_j W_{i+k}] + \sum_{j=i}^{i+k} \mathrm{E}[Y_j S_{i+k}]
\end{aligned}$$

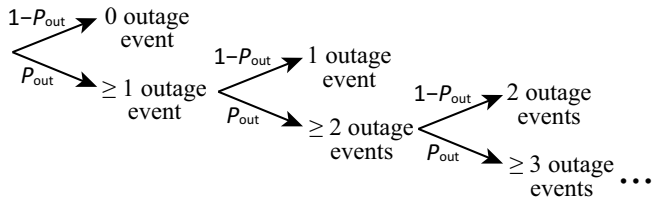


Fig. 10. The probability of $k$ successive outage events.

$$= \sum_{j=i}^{i+k} \mathrm{E}[Y_j W_{i+k}] + (k+1)\mathrm{E}[Y]\mathrm{E}[S]. \tag{51}$$

$$\begin{aligned}
\mathrm{E}[\tilde{Y}^2] &= \mathrm{E}[\tilde{Y}_i^2] \\
&= \mathrm{E}\left[\left(\sum_{j=i}^{i+k} Y_j\right)^2\right] \\
&= \mathrm{E}\left[\sum_{j=i}^{i+k} Y_j^2 + 2\sum_{j=i}^{i+k-1}\sum_{j'=j+1}^{i+k} Y_j Y_{j'}\right] \\
&= (k+1)\mathrm{E}[Y^2] + 2\sum_{j=i}^{i+k-1}\sum_{j'=j+1}^{i+k} \mathrm{E}[Y_j]\mathrm{E}[Y_{j'}] \\
&= (k+1)\mathrm{E}[Y^2] + k(k+1)(\mathrm{E}[Y])^2 \\
&= (k+1)\left(\mathrm{E}[Y^2] + k(\mathrm{E}[Y])^2\right).
\end{aligned} \tag{52}$$

$$\mathrm{E}[\tilde{Y}] = \mathrm{E}[\tilde{Y}_i] = \mathrm{E}\left[\sum_{j=i}^{i+k} Y_j\right] = \sum_{j=i}^{i+k} \mathrm{E}\left[Y_j\right] = (k+1)\mathrm{E}[Y]. \tag{53}$$

## Appendix B
## Proof of Proposition 1

To derive the average AoI for the system in the stable states, we need to take the probability of the outage events successively occurring $k$ times into account. As illustrated in Fig. 10, given an outage probability $P_{\text{out}}$, the probability of no outage event is $(1-P_{\text{out}})$, and hence $(1-P_{\text{out}})$ corresponds to the event space without outage event. The remaining event space $P_{\text{out}}$ corresponds to one or more than one outage events. Then, we can further divide the event space of $k \geq 1$ into the event spaces of $k=1$ and of $k \geq 2$ with the probabilities being $(1-P_{\text{out}})$ and $P_{\text{out}}$, respectively. By recursively dividing the event spaces, we can obtain the probability of successively occurring $k$ outage events as $P_{\text{out}}^k(1-P_{\text{out}})$. For a sufficiently large $N_T$ of successful transmissions, the number of $k$ successive outage events is $N_T \cdot P_{\text{out}}^k(1-P_{\text{out}})$. Furthermore, the average area of trapezoids with $k$ outage events is

$$\begin{aligned}
\mathrm{E}[\tilde{Q}] &= \Delta_{(k)}\mathrm{E}[\tilde{Y}] \\
&= \Delta_{(k)}\mathrm{E}\left[\sum_{j=i}^{i+k} Y_j\right] \\
&= \Delta_{(k)}\sum_{j=i}^{i+k} \mathrm{E}\left[Y_j\right] \\
&= \Delta_{(k)}(k+1)\mathrm{E}\left[Y\right].
\end{aligned} \tag{54}$$

Therefore, the summation of all $\tilde{Q}_i$ for $k$ successive outage events in $N_T$ successful transmissions is $N_T P_{\text{out}}^k(1-P_{\text{out}}) \cdot \Delta_{(k)}(k+1)\mathrm{E}\left[Y\right]$. Hence, the total area under $\Delta(t)$ in $N_T$ successful transmissions is given by $\sum_{k=0}^{\infty} N_T P_{\text{out}}^k(1-P_{\text{out}}) \cdot \Delta_{(k)}(k+1)\mathrm{E}\left[Y\right]$. Likewise, we can obtain the total time for $N_T$ successful transmissions as $\sum_{k=0}^{\infty} N_T P_{\text{out}}^k(1-P_{\text{out}}) \cdot (k+1)\mathrm{E}\left[Y\right]$. Consequently, the average AoI for the system with outage events is

$$\begin{aligned}
\Delta &= \frac{\sum_{k=0}^{\infty} N_T P_{\text{out}}^k(1-P_{\text{out}}) \cdot \Delta_{(k)}(k+1)\mathrm{E}\left[Y\right]}{\sum_{k=0}^{\infty} N_T P_{\text{out}}^k(1-P_{\text{out}}) \cdot (k+1)\mathrm{E}\left[Y\right]} \\
&= \frac{\sum_{k=0}^{\infty} P_{\text{out}}^k(k+1)\Delta_{(k)}}{\sum_{k=0}^{\infty} P_{\text{out}}^k(k+1)} \\
&= \frac{\sum_{k=0}^{\infty} P_{\text{out}}^k(k+1)\Delta_{(k)}}{1/(1-P_{\text{out}})^2} \qquad (55) \\
&= (1-P_{\text{out}})^2 \sum_{k=0}^{\infty} P_{\text{out}}^k(k+1)\Delta_{(k)}, \qquad (56)
\end{aligned}$$

where (55) follows according to [30, Eq. (0.231.2)] for $P_{\text{out}} < 1$. Obviously, when $P_{\text{out}} = 1$, the transmission always fails and hence the average AoI becomes $\infty$.

This finishes the proof of *Proposition 1*.

## Appendix C
## Proof of Proposition 2

Consider

$$\begin{aligned}
\mathrm{E}[Y] &= \int_0^{\infty} y f_Y(y) dy \\
&= \int_0^{\infty} y \int_0^{\infty} f_{Y|W}(y|w) f_W(w) dw dy \\
&= \int_0^{\infty} f_W(w) dw \int_0^{\infty} y f_{Y|W}(y|w) dy \\
&= \int_0^{\infty} f_W(w) \mathrm{E}[Y|W=w] dw.
\end{aligned} \tag{57}$$

Therefore, we have

$$\begin{aligned}
\mathrm{E}[Y_j] &= \int_0^{\infty} f_{W_{i-1}}(w) \mathrm{E}[Y_j|W_{i-1}=w] dw \\
&= \int_0^{\infty} f_{W_{i+k}}(w) \mathrm{E}[Y_j|W_{i+k}=w] dw.
\end{aligned} \tag{58}$$

On the one hand, $W_{i-1}$ is independent of $Y_j$, i.e., $\mathrm{E}[Y_j|W_{i-1}=w] = \mathrm{E}[Y_j]$, because $i-1 < j$. On the other hand, if $Y_j$ is larger, it means that the $j$-th packet arrives later, and recursively the $(i+k)$-th packet also arrives later. Hence, the system has more time to serve the packets in the queue, and the waiting time $W_{i+k}$ becomes smaller. Consequently, the smaller $W_{i+k}$, the larger $\mathrm{E}[Y_j|W_{i+k}=w]$, i.e.,

$$\mathrm{E}[Y_j|W_{i+k}=w] < \mathrm{E}[Y_j|W_{i+k}=w'], \text{ for any } w > w'. \tag{59}$$

Obviously, $\mathrm{E}[Y_j|W_{i+k}=w]$ is a monotonically decreasing function with respect to $w$. Moreover, $\mathrm{E}[Y_j|W_{i+k}=w]$ must have some values larger than $\mathrm{E}[Y_j]$ and some other values smaller than $\mathrm{E}[Y_j]$. Otherwise, let us assume that

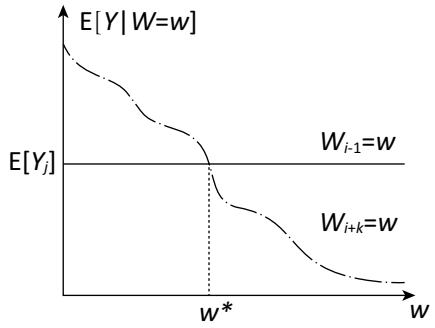


Fig. 11. The tendencies of $\mathrm{E}[Y_j|W_{i-1}=w]$ and $\mathrm{E}[Y_j|W_{i+k}=w]$.

$\mathrm{E}[Y_j] \geq \mathrm{E}[Y_j|W_{i+k}=w]$ always holds. Since $f_{W_{i-1}}(w) = f_{W_{i+k}}(w) = f_W(w) \geq 0$, we have

$$f_{W_{i-1}}(w)\mathrm{E}[Y_j|W_{i-1}=w] \geq f_{W_{i+k}}(w)\mathrm{E}[Y_j|W_{i+k}=w] \quad (60)$$

$$\int_0^\infty f_{W_{i-1}}(w)\mathrm{E}[Y_j|W_{i-1}=w]dw > \int_0^\infty f_{W_{i+k}}(w)\mathrm{E}[Y_j|W_{i+k}=w]dw, \quad (61)$$

where the equality of (61) cannot hold because $\mathrm{E}[Y_j|W_{i+k}=w]$ is monotonically decreasing. Clearly, (61) conflicts with (58), and hence the assumption that $\mathrm{E}[Y_j] \geq \mathrm{E}[Y_j|W_{i+k}=w]$ for all $w$ is incorrect. Similarly, we can also prove that $\mathrm{E}[Y_j] \leq \mathrm{E}[Y_j|W_{i+k}=w]$ cannot always hold. Consequently, the tendencies of $\mathrm{E}[Y_j|W_{i+k}=w]$ and $\mathrm{E}[Y_j|W_{i-1}=w]$ are like the curves illustrated in Fig. 11, where the convexity or concavity of $\mathrm{E}[Y_j|W_{i+k}=w]$ does not matter.

In addition, due to the monotonicity of $\mathrm{E}[Y_j|W_{i+k}=w]$, the two curves must have one and only one cross point $(w^*, \mathrm{E}[Y_j])$, and

$$\mathrm{E}[Y_j|W_{i+k}=w] > \mathrm{E}[Y_j|W_{i-1}=w], \quad \text{for } 0 \leq w < w^*, \quad (62)$$

$$\mathrm{E}[Y_j|W_{i+k}=w] < \mathrm{E}[Y_j|W_{i-1}=w], \quad \text{for } w > w^*. \quad (63)$$

Furthermore, since $f_{W_{i-1}}(w) = f_{W_{i+k}}(w) = f_W(w) \geq 0$, we have

$$f_{W_{i+k}}(w)\mathrm{E}[Y_j|W_{i+k}=w] > f_{W_{i-1}}(w)\mathrm{E}[Y_j|W_{i-1}=w], \quad \text{for } 0 \leq w < w^*, \quad (64)$$

$$f_{W_{i+k}}(w)\mathrm{E}[Y_j|W_{i+k}=w] < f_{W_{i-1}}(w)\mathrm{E}[Y_j|W_{i-1}=w], \quad \text{for } w > w^*. \quad (65)$$

Now, we introduce the following lemma to bound $\mathrm{E}[Y_jW_{i+k}]$.

*Lemma 1* (*integral scaling lemma*): If two functions $g_1(w)$ and $g_2(w)$ satisfy

$$\int_0^\infty g_1(w)dw = \int_0^\infty g_2(w)dw, \quad (66)$$

$$g_2(w) > g_1(w), \quad \text{for } 0 \leq w < w^*, \quad (67)$$

$$g_2(w) < g_1(w), \quad \text{for } w > w^*, \quad (68)$$

then the following inequality holds

$$\int_0^\infty w g_2(w)dw < \int_0^\infty w g_1(w)dw. \quad (69)$$

The proof of *Lemma 1* is presented in Appendix D. Let $g_1(w) = f_{W_{i-1}}(w)\mathrm{E}[Y_j|W_{i-1}=w]$ and $g_2(w) = f_{W_{i+k}}(w)\mathrm{E}[Y_j|W_{i+k}=w]$, and hence we have

$$\int_0^\infty w f_{W_{i+k}}(w)\mathrm{E}[Y_j|W_{i+k}=w]dw < \int_0^\infty w f_{W_{i-1}}(w)\mathrm{E}[Y_j|W_{i-1}=w]dw. \quad (70)$$

Moreover, consider

$$\begin{aligned}\mathrm{E}[YW] &= \int_0^\infty \int_0^\infty yw f_{Y,W}(y,w)dydw \\ &= \int_0^\infty \int_0^\infty yw f_{Y|W}(y|w) f_W(w)dydw \\ &= \int_0^\infty w f_W(w)dw \int_0^\infty y f_{Y|W}(y|w)dy \\ &= \int_0^\infty w f_W(w)\mathrm{E}[Y|W=w]dw. \end{aligned} \quad (71)$$

By substituting (71) into (70), we can finally obtain

$$\mathrm{E}[Y_jW_{i+k}] < \mathrm{E}[Y_jW_{i-1}]. \quad (72)$$

This finishes the proof of *Proposition 2*.

## Appendix D
## Proof of Lemma 1

Calculate the integrals as (73)-(75) on the top of the next page, where (74) follows since $w^* > w > 0$, $g_2(w) - g_1(w) > 0$ in the interval $(0, w^*)$, and $w > w^* > 0$, $g_1(w) - g_2(w) > 0$ in the interval $(w^*, \infty)$. This finishes the proof of *Lemma 1*.

*Lemma 1* has an intuitive explanation as follows. Two functions having the same integral value mean that the areas under the functions are equal. If the two functions have one and only one cross point at $(w^*, g_i(w^*))$, one of the functions must has larger area on the left side of the cross point, and smaller area on the right side. Then, $w \cdot g_i(w)$ is to scale $g_i(w)$ by $w$, and the area for $w < w^*$ is enlarged less than the area for $w^* < w$. Consequently, the curve higher than another when $w^* < w$ will have larger area in $[0, \infty)$ after scaled by $w$. To help better understand this lemma, we call it *integral scaling lemma*.

## References


[1] Y. Sun, I. Kadota, R. Talak, and E. Modiano, *Age of Information: A New Metric for Information Freshness*, ser. Synthesis Lectures on Communication Networks, R. Srikant, Ed. Williston, VT: Morgan & Claypool Publishers, 2019.

[2] S. Kaul, M. Gruteser, V. Rai, and J. Kenney, "Minimizing age of information in vehicular networks," in *the 8th Annual IEEE Communications Society Conference on Sensor, Mesh and Ad Hoc Communications and Networks*, Salt Lake City, UT, Jun. 2011, pp. 350–358.

[3] S. Zhang, H. Zhang, L. Song, Z. Han, and H. V. Poor, "Sensing and communication tradeoff design for AoI minimization in a cellular internet of UAVs," in *IEEE International Conference on Communications*, Dublin, Ireland, Jun. 2020.

[4] G. Ahani, D. Yuan, and Y. Zhao, "Age-optimal UAV scheduling for data collection with battery recharging," *IEEE Communications Letters*, vol. 25, no. 4, pp. 1254–1258, 2021.

$$\int_0^{\infty} g_2(w)dw = \int_0^{\infty} g_1(w)dw \tag{73}$$

$$\int_0^{w^*} g_2(w)dw + \int_{w^*}^{\infty} g_2(w)dw = \int_0^{w^*} g_1(w)dw + \int_{w^*}^{\infty} g_1(w)dw$$

$$\int_0^{w^*} g_2(w)dw - \int_0^{w^*} g_1(w)dw = \int_{w^*}^{\infty} g_1(w)dw - \int_{w^*}^{\infty} g_2(w)dw$$

$$\int_0^{w^*} w^* g_2(w)dw - \int_0^{w^*} w^* g_1(w)dw = \int_{w^*}^{\infty} w^* g_1(w)dw - \int_{w^*}^{\infty} w^* g_2(w)dw$$

$$\int_0^{w^*} w g_2(w)dw - \int_0^{w^*} w g_1(w)dw < \int_{w^*}^{\infty} w g_1(w)dw - \int_{w^*}^{\infty} w g_2(w)dw \tag{74}$$

$$\int_0^{w^*} w g_2(w)dw + \int_{w^*}^{\infty} w g_2(w)dw < \int_0^{w^*} w g_1(w)dw + \int_{w^*}^{\infty} w g_1(w)dw$$

$$\int_0^{\infty} w g_2(w)dw < \int_0^{\infty} w g_1(w)dw. \tag{75}$$


[5] Y. Gu, H. Chen, Y. Zhou, Y. Li, and B. Vucetic, "Timely status update in internet of things monitoring systems: An age-energy tradeoff," *IEEE Internet of Things Journal*, vol. 6, no. 3, pp. 5324–5335, 2019.

[6] Y. Gu, H. Chen, C. Zhai, Y. Li, and B. Vucetic, "Minimizing age of information in cognitive radio-based IoT systems: Underlay or overlay?" *IEEE Internet of Things Journal*, vol. 6, no. 6, pp. 10 273–10 288, 2019.

[7] Z. Ling, F. Hu, H. Zhang, Z. Han, and H. V. Poor, "Distributionally robust optimization for peak age of information minimization in E-health IoT," in *IEEE International Conference on Communications*, Montreal, Canada, Jun. 2021.

[8] Cisco, "Cisco annual internet report (2018–2023) white paper," Tech. Rep., Mar. 2020.

[9] K. Chen and L. Huang, "Age-of-information in the presence of error," in *IEEE International Symposium on Information Theory (ISIT)*, Barcelona, Spain, Jul. 2016, pp. 2579–2583.

[10] A. Arafa, J. Yang, S. Ulukus, and H. V. Poor, "Online timely status updates with erasures for energy harvesting sensors," in *the 56th Annual Allerton Conference on Communication, Control, and Computing (Allerton)*, Monticello, IL, Oct. 2018, pp. 966–972.

[11] C. Kam, S. Kompella, G. D. Nguyen, J. E. Wieselthier, and A. Ephremides, "On the age of information with packet deadlines," *IEEE Transactions on Information Theory*, vol. 64, no. 9, pp. 6419–6428, Sep. 2018.

[12] S. Zhang, H. Zhang, Z. Han, H. V. Poor, and L. Song, "Age of information in a cellular internet of UAVs: Sensing and communication trade-off design," *IEEE Transactions on Wireless Communications*, vol. 19, no. 10, pp. 6578–6592, Oct. 2020.

[13] W. Lin, L. Li, J. Yuan, Z. Han, M. Juntti, and T. Matsumoto, "Cooperative lossy communications in unmanned aerial vehicle networks: Age-of-information with outage probability," *IEEE Transactions on Vehicular Technology*, vol. 70, no. 10, pp. 10 105–10 120, Oct. 2021.

[14] Z. Ling, F. Hu, H. Zhang, and Z. Han, "Age of information minimization in healthcare IoT using distributionally robust optimization," *IEEE Internet of Things Journal (Early Access)*, Feb. 2022.

[15] M. Moltafet, M. Leinonen, and M. Codreanu, "On the age of information in multi-source queueing models," *IEEE Transactions on Communications*, vol. 68, no. 8, pp. 5003–5017, Aug. 2020.

[16] S. K. Kaul and R. D. Yates, "Timely updates by multiple sources: The M/M/1 queue revisited," in *54th Annual Conference on Information Sciences and Systems (CISS)*, Princeton, NJ, Mar. 2020, pp. 1–6.

[17] L. Huang and E. Modiano, "Optimizing age-of-information in a multi-class queueing system," in *IEEE International Symposium on Information Theory (ISIT)*, Hong Kong, China, Jun. 2015, pp. 1681–1685.

[18] G. Kramer, M. Gastpar, and P. Gupta, "Cooperative strategies and capacity theorems for relay networks," *IEEE Transactions on Information Theory*, vol. 51, no. 9, pp. 3037–3063, Aug. 2005.

[19] X. Zhou, M. Cheng, X. He, and T. Matsumoto, "Exact and approximated outage probability analyses for decode-and-forward relaying system allowing intra-link errors," *IEEE Transactions on Wireless Communications*, vol. 13, no. 12, pp. 7062–7071, Dec. 2014.

[20] S. Qian, J. He, M. Juntti, and T. Matsumoto, "Fading correlations for wireless cooperative communications: Diversity and coding gains," *IEEE Access*, vol. 5, pp. 8001–8016, 2017.

[21] J. He, V. Tervo, S. Qian, Q. Xue, M. Juntti, and T. Matsumoto, "Performance analysis of lossy decode-and-forward for non-orthogonal MARCs," *IEEE Transactions on Wireless Communications*, vol. 17, no. 3, pp. 1545–1558, Mar. 2018.

[22] H. Zhang and Z. Zhang, "Outage analysis and learning-based relay selection for opportunistic lossy forwarding relaying systems," *IEEE Access*, vol. 8, pp. 104 386–104 395, Jun. 2020.

[23] J. He, V. Tervo, X. Zhou, X. He, S. Qian, M. Cheng, M. Juntti, and T. Matsumoto, "A tutorial on lossy forwarding cooperative relaying," *IEEE Communications Surveys & Tutorials*, vol. 21, no. 1, pp. 66–87, First quarter 2018.

[24] W. Lin, S. Qian, and T. Matsumoto, "Lossy-forward relaying for lossy communications: Rate-distortion and outage probability analyses," *IEEE Transactions on Wireless Communications*, vol. 18, no. 8, pp. 3974–3986, Aug. 2019.

[25] W. Lin, Q. Xue, J. He, M. Juntti, and T. Matsumoto, "Rate-distortion and outage probability analyses for single helper assisted lossy communications," *IEEE Transactions on Vehicular Technology*, vol. 68, no. 11, pp. 10 882–10 894, Nov. 2019.

[26] C. E. Shannon, "A mathematical theory of communication," *Bell System Technical Journal*, vol. 27, no. 3, pp. 379–423, Jul. 1948.

[27] ——, "Coding theorems for a discrete source with a fidelity criterion," *IRE Nat. Conv. Rec*, vol. 4, no. 1, pp. 142–163, Mar. 1959.

[28] A. Kosta, N. Pappas, and V. Angelakis, *Age of Information: A New Concept, Metric, and Tool*. Hanover, MA: now Publishers Inc., 2017.

[29] A. Papoulis and S. U. Pillai, *Probability, random variables, and stochastic processes*, the 4th ed. New York: McGraw-Hill, 2002.

[30] I. S. Gradshteyn and I. M. Ryzhik, *Table of integrals, series, and products*, the 7th ed., A. Jeffrey and D. Zwillinger, Eds. Burlington, MA: Academic Press, 2007.

[31] C. Robert and G. Casella, *Monte Carlo statistical methods*, the 2nd ed. Springer Science & Business Media, 2004.

[32] T. M. Cover and J. A. Thomas, *Elements of information theory*. John Wiley & Sons, 2012.

[33] A. El Gamal and Y.-H. Kim, *Network information theory*. Cambridge University Press, 2011.

**Wensheng Lin** (S'17-M'20) received the B.Eng. degree in communication engineering, and the M.Eng. degree in electronic and communication engineering from Northwestern Polytechnical University, Xi'an, China, in 2013 and 2016, respectively, and the Ph.D. degree in information science from Japan Advanced Institute of Science and Technology (JAIST), Ishikawa, Japan, in 2019. He is currently an Associate Professor with the School of Electronics and Information, Northwestern Polytechnical University, Xi'an, China. His research interests include network information theory, distributed source coding, and Age of Information.

**Lixin Li** (M'12) received the B.S., the M.S. and the Ph.D. degrees from Northwestern Polytechnical University (NPU), Xi'an, China, in 2001, 2004, and 2008, respectively. He was a Postdoctoral Fellow with NPU from 2009 to 2011. In 2017, He was a Visiting Scholar with the University of Houston, Texas. He is currently a Professor with the School of Electronics and Information, NPU. He has authored or coauthored more than 150 peer-reviewed papers in many prestigious journals and conferences, and he holds 20 patents. His current research interests include wireless communications, game theory, and machine learning. He received the 2016 NPU Outstanding Young Teacher Award, which is the highest research and education honors for young faculties in NPU. He was an exemplary reviewer for IEEE Transactions on Communications in 2020.

**Jinhong Yuan** (M'02–SM'11–F'16) received the B.E. and Ph.D. degrees in electronics engineering from the Beijing Institute of Technology, Beijing, China, in 1991 and 1997, respectively. From 1997 to 1999, he was a Research Fellow with the School of Electrical Engineering, University of Sydney, Sydney, Australia. In 2000, he joined the School of Electrical Engineering and Telecommunications, University of New South Wales, Sydney, Australia, where he is currently a Professor and Head of Telecommunication Group with the School. He has published two books, five book chapters, over 300 papers in telecommunications journals and conference proceedings, and 50 industrial reports. He is a co-inventor of one patent on MIMO systems and two patents on low-density-parity-check codes. He has co-authored four Best Paper Awards and one Best Poster Award, including the Best Paper Award from the IEEE International Conference on Communications, Kansas City, USA, in 2018, the Best Paper Award from IEEE Wireless Communications and Networking Conference, Cancun, Mexico, in 2011, and the Best Paper Award from the IEEE International Symposium on Wireless Communications Systems, Trondheim, Norway, in 2007. He is an IEEE Fellow and currently serving as an Associate Editor for the IEEE Transactions on Wireless Communications and IEEE Transactions on Communications. He served as the IEEE NSW Chapter Chair of Joint Communications/Signal Processions/Ocean Engineering Chapter during 2011-2014 and served as an Associate Editor for the IEEE Transactions on Communications during 2012-2017. His current research interests include error control coding and information theory, communication theory, and wireless communications.

**Zhu Han** (S'01–M'04-SM'09-F'14) received the B.S. degree in electronic engineering from Tsinghua University, in 1997, and the M.S. and Ph.D. degrees in electrical and computer engineering from the University of Maryland, College Park, in 1999 and 2003, respectively.

From 2000 to 2002, he was an R&D Engineer of JDSU, Germantown, Maryland. From 2003 to 2006, he was a Research Associate at the University of Maryland. From 2006 to 2008, he was an assistant professor at Boise State University, Idaho. Currently, he is a John and Rebecca Moores Professor in the Electrical and Computer Engineering Department as well as in the Computer Science Department at the University of Houston, Texas. His research interests include wireless resource allocation and management, wireless communications and networking, game theory, big data analysis, security, and smart grid. Dr. Han received an NSF Career Award in 2010, the Fred W. Ellersick Prize of the IEEE Communication Society in 2011, the EURASIP Best Paper Award for the Journal on Advances in Signal Processing in 2015, IEEE Leonard G. Abraham Prize in the field of Communications Systems (best paper award in IEEE JSAC) in 2016, and several best paper awards in IEEE conferences. Dr. Han was an IEEE Communications Society Distinguished Lecturer from 2015-2018, AAAS fellow since 2019, and ACM distinguished Member since 2019. Dr. Han is a 1% highly cited researcher since 2017 according to Web of Science. Dr. Han is also the winner of the 2021 IEEE Kiyo Tomiyasu Award, for outstanding early to mid-career contributions to technologies holding the promise of innovative applications, with the following citation: "for contributions to game theory and distributed management of autonomous communication networks."

**Markku Juntti** (S'93–M'98–SM'04–F'20) received his M.Sc. (EE) and Dr.Sc. (EE) degrees from University of Oulu, Oulu, Finland in 1993 and 1997, respectively.

Dr. Juntti was with University of Oulu in 1992–98. In academic year 1994–95, he was a Visiting Scholar at Rice University, Houston, Texas. In 1999–2000, he was a Senior Specialist with Nokia Networks in Oulu, Finland. Dr. Juntti has been a professor of communications engineering since 2000 at University of Oulu, Centre for Wireless Communications (CWC), where he leads the Communications Signal Processing (CSP) Research Group. He also serves as Head of CWC – Radio Technologies (RT) Research Unit. His research interests include signal processing for wireless networks as well as communication and information theory. He is an author or co-author in almost 500 papers published in international journals and conference records as well as in books *Wideband CDMA for UMTS* in 2000–2010, *Handbook of Signal Processing Systems* in 2013 and 2018 and *5G Wireless Technologies* in 2017. Dr. Juntti is also an Adjunct Professor at Department of Electrical and Computer Engineering, Rice University, Houston, Texas, USA.

Dr. Juntti was an Editor of IEEE TRANSACTIONS ON COMMUNICATIONS and an Associate Editor for IEEE TRANSACTIONS ON VEHICULAR TECHNOLOGY. He was Secretary of IEEE Communication Society Finland Chapter in 1996–97 and the Chairman for years 2000–01. He has been Secretary of the Technical Program Committee (TPC) of the 2001 IEEE International Conference on Communications (ICC), and the Chair or Co-Chair of the Technical Program Committee of several conferences including 2006 and 2021 IEEE International Symposium on Personal, Indoor and Mobile Radio Communications (PIMRC), the Signal Processing for Communications Symposium of IEEE Globecom 2014, Symposium on Transceivers and Signal Processing for 5G Wireless and mm-Wave Systems of IEEE GlobalSIP 2016, ACM NanoCom 2018, and 2019 International Symposium on Wireless Communication Systems (ISWCS). He has also served as the General Chair of 2011 IEEE Communication Theory Workshop (CTW 2011) and 2022 IEEE Workshop on Signal Processing Advances in Wireless Communications (SPAWC).

**Tad Matsumoto** (S'84-M'98-F'10-LF'21) received his B.S. and M.S. degrees in electrical engineering, and his Ph.D. degree in electrical engineering, all from Keio University, Yokohama, Japan, in 1978, 1980, and 1991, respectively. He joined Nippon Telegraph and Telephone Corporation (NTT), in 1980, where he was involved in a lot of research and development projects mobile wireless communications systems. In 1992, he transferred to NTT DoCoMo, where he researched on code-division multiple-access techniques for mobile communication systems. In 1994, he transferred to NTT America, where he served as a Senior Technical Advisor of a joint project between NTT and NEXTEL Communications. In 1996, he returned to NTT DoCoMo, where he served as the Head of the Radio Signal Processing Laboratory, until 2001. He researched on adaptive signal processing, multiple-input multiple-output turbo signal detection, interference cancellation, and space-time coding techniques for broadband mobile communications. In 2002, he moved to the University of Oulu, Finland, where he served as a Professor at Centre for Wireless Communications. In 2006, he has served as a Visiting Professor with the Ilmenau University of Technology, Ilmenau, Germany, supported by the German MERCATOR Visiting Professorship Program. Since 2007, he has been serving as a Professor with the Japan Advanced Institute of Science and Technology (JAIST), Japan, while also keeping a cross-appointment position with the University of Oulu. After his retirement from JAIST, he moved to IMT-Atlantic, France, where he is serving as an invited professor. He is also Professor Emeritus of both JAIST and University of Oulu.

Prof. Matsumoto is a member of the IEICE. He has led a lot of projects supported by the Academy of Finland, European FP7, and the Japan Society for the Promotion of Science and Japanese private companies. He has been appointed as a Finland Distinguished Professor, from 2008 to 2012, supported by Finnish National Technology Agency (Tekes) and Finnish Academy, under which he preserves the rights to participate in and apply for European and Finnish National Projects. He was a recipient of IEEE VTS Outstanding Service Award, in 2001, Nokia Foundation Visiting Fellow Scholarship Award, in 2002, IEEE Japan Council Award for Distinguished Service to the Society, in 2006, the IEEE Vehicular Technology Society James R. Evans Avant Garde Award, in 2006, Thuringen State Research Award for Advanced Applied Science, in 2006, the 2007 Best Paper Award of the Institute of Electrical, Communication, and Information Engineers of Japan, in 2008, Telecom System Technology Award from the Telecommunications Advancement Foundation, in 2009, IEEE Communication Letters Exemplary Reviewer, in 2011, Nikkei Wireless Japan Award, in 2013, IEEE VTS Recognition for Outstanding Distinguished Lecturer, in 2016, and IEEE TRANSACTIONSON COMMUNICATIONS Exemplary Reviewer, in 2018. He has been serving as an IEEE Vehicular Technology Distinguished Speaker, since 2016.